Cell sorting by differential cell motility: a model for pattern formation in Dictyostelium

Umeda, Tamiki

Inouye, Kei

(Citation)
Journal of Theoretical Biology,226(2):215-224

(Issue Date)
2004-01-24

(Resource Type)
journal article

(Version)
Accepted Manuscript

(URL)
https://hdl.handle.net/20.500.14094/90000252

Cell sorting by differential cell motility: a model for pattern formation in *Dictyostelium*

Tamiki Umeda [a,*], Kei Inouye [b]

[a] *Faculty of Maritime Sciences, Kobe University, Kobe 658-0022, Japan*

[b] *Department of Botany, Division of Biological Science, Graduate School of Science, Kyoto University, Kyoto 606-8502, Japan*

Abstract

In the slug stage of the cellular slime mold *Dictyostelium discoideum*, prespore cells and four types of prestalk cells show a well-defined spatial distribution in a migrating slug. We have developed a continuous mathematical model for the distribution pattern of these cell types based on the balance of force in individual cells. In the model, cell types are assumed to have different properties in cell motility, i.e., different motive force, the rate of resistance against cell movement, and diffusion coefficient. Analysis of the stationary solution of the model shows that combination of these parameters and slug speed determines the 3-dimensional shape of a slug and cell distribution pattern within it. Based on experimental data of slug motive force and velocity measurements, appropriate sets of parameters were chosen so that the cell-type distribution at stationary state matches the distribution in real slugs. With these parameters, we performed numerical calculation of the model in 2-dimensional space using a moving particle method. The results reproduced many of the basic features of slug morphogenesis, i.e., cell sorting, translocation of the prestalk region, elongation of the slug, and its steady migration.

Key words: slime mold, cell movement, morphogenesis, simulation, mathematical model

* Corresponding author.
emai: umeda@maritime.kobe-u.ac.jp

1 Introduction

Migration of differentiated cells is an important process in multicellular development. Besides causing rearrangement of cells in a tissue, it is directly involved in the morphogenesis. With its very simple structure, the slug of the cellular slime mold *Dictyostelium discoideum* is an ideal model system for theoretical and experimental studies of morphogenetic cell movement (for reviews, see Bonner (1994); Dormann et al. (2000)).

Upon starvation, amoebae of *D. discoideum* aggregate to form a mound of cells, which then elongate to become a finger like structure called a slug. Under humid conditions, the slug falls on the substratum and starts to migrate. The slug consists of two major cell types; prestalk cells are distributed mostly in the front quarter of the slug and prespore cells occupy the remaining part. Within the prestalk cells, four subtypes have been identified (pstA, pstB, pstAB, and pstO cells), which differ from each other in the transcriptional activities of prestalk specific genes and show well-defined spatial distributions in a slug (Williams et al., 1989). Experiments with labeled cells indicate that the spatial pattern of these cell types seen in the slug is generated by rearrangement of the cells that have differentiated within the mound (Tasaka and Takeuchi, 1981; Early et al., 1995; Araki et al., 1997).

Two types of models have been proposed for slug movement and cell sorting. Continuous models use equations similar to those in fluid dynamics to simulate the movement of a cell mass (Dormann et al., 1998; Vasiev and Weijer, 1999). These approaches have successfully reproduced the process of slug development, but the relationship between the model parameters and physical properties of cells is unclear. On the other hand, individual-based models consider the properties of individual cells, such as active force to chemical source, cell size, stiffness, and adhesion between cells (Yi Jiang et al., 1998; Marée et al., 1999; Pálsson and Othmer, 2000). However, the difficulty in the analysis of the models makes numerical simulations the only method to evaluate the effects of individual parameters.

For better understanding of the mechanism of cell sorting and tissue movement, we consider it important to adequately formulate the mechanical aspects of the phenomena in the model. In the previous studies (Umeda, 1989; Umeda and Inouye, 1999), we have developed continuous models for cell sorting and slug movement based on the balance of forces in individual cells capable of active movement by their own motive force. Analytical and numerical study of the models have shown that the difference in motive force among cell types plays important roles both in producing cell distribution patterns within slugs and in forming the slug shape. However, only two cell types were postulated in the models and limited situations were considered in numerical analysis

because of the difficulty in computation.

In this study, we extend the model to include more than two types of cells which may have different motive force, different intrinsic resistance against cell movement, and different diffusion coefficient. We will first analyze the cell-type distribution and slug shape at stationary state, then investigate the process of slug development by numerical calculation of the model equations using a moving particle method. The results indicate that the distribution patterns of the prestalk subtypes and prespore cells within slugs can be explained by the difference in the mechanical parameters among these cell types.

2 Model

We consider a slug consisting of several cell types, which will be denoted type-α, type-β, etc in the following. The cell number of each cell type as well as their cellular identities are assumed to be unchanged. Though it has been shown that the movement of individual cells within slugs is controlled by intercellular signaling substances, we here neglect the details of chemical signaling and employ the following simplified model. First, a single pacemaker cell or a single pacemaker region is postulated within the slug. The position of the pacemaker is assumed to move with the averaged velocity of the surrounding cells. Second, in average each cell is assumed to exert motive force in the direction of the pacemaker. These assumptions imply that chemotactic signals emanating from the pacemaker are propagated uniformly in the slug and their speed is sufficiently faster than the speed of cells (Umeda and Inouye, 1999).

The movement of a type-α cell located at position $\mathbf{x}(t)$ at time t will be determined by the balance between motive force, the intrinsic resistance of the cell against cell movement, and the force from the surrounding cells (which will be called external force). The magnitude of the motive force (f_α) is assumed to be a constant depending on cell type and, as stated above, the force vector is directed towards the pacemaker at position $\mathbf{x}_\mathrm{p}(t)$. The intrinsic resistance is considered to be mostly due to the viscoelasticity of the cytoplasm. We assume that this force is proportional to the cell speed $\mathbf{V}_\alpha$ and its coefficient a_α is a constant specific to cell type. The external force can be expressed in the form of the gradient of pressure p, which is determined so that the density of the cells ρ is uniform throughout the slug. In addition, random force $\boldsymbol{\xi}_\alpha(t)$ is considered in the model. Fluctuations of the motive force (both magnitude and direction) and deviations of the external force from its average will be included in this force. Under these assumptions, the force balance equation of

a type-α cell can be written as:

$$f_\alpha \frac{\mathbf{x}_\mathrm{p} - \mathbf{x}}{|\mathbf{x}_\mathrm{p} - \mathbf{x}|} - a_\alpha \mathbf{V}_\alpha - \frac{1}{\rho}\nabla p + \boldsymbol{\xi}_\alpha = 0. \tag{1}$$

Let us consider a small volume element at position $\mathbf{x}$ within the slug. This volume element may contain more than one cell types, and let $n_\alpha(\mathbf{x}, t)$ denote the fraction of type-α cells in this volume element at time t. The net movement rate, or the "flux density" $\mathbf{J}_\alpha$, of type-α cells consists of the flow caused by oriented movement of type-α cells with the average velocity $\langle \mathbf{V}_\alpha \rangle$ and the flow caused by random cell movement. We assume that the latter can be described as a process of diffusion, the coefficient of which being a cell-type-dependent constant D_α (see Eq. (A.1), (A.2) of Appendix A).

To obtain the spatial distribution of each cell type in the slug, it is convenient to consider the velocity of the cell mass at each position of the slug and the flux relative to the movement of the cell mass. The velocity of the cell mass $\mathbf{v}(\mathbf{x}, t)$ at position $\mathbf{x}$ at time t is a weighted mean velocity of all cell types in the volume element, and defined by $\mathbf{v}(\mathbf{x}, t) = (1/\rho) \sum_\alpha \mathbf{J}_\alpha$. Then the relative flux density $\mathbf{J}_\alpha^\mathrm{rel}$ of type-α cells is given by

$$\mathbf{J}_\alpha^\mathrm{rel} = \mathbf{J}_\alpha - \mathbf{J}_\alpha^*, \tag{2}$$

where $\mathbf{J}_\alpha^* = \rho n_\alpha \mathbf{v}$ is the flux density of type-α cells as they move with the cell mass. The changes in the fraction of type-α cells n_α can be calculated from $\mathbf{v}$ and $\mathbf{J}_\alpha^\mathrm{rel}$ using the equation of continuity (see Appendix A).

The boundary of the slug moves with the velocity $\mathbf{v}$. If we neglect the force from the substratum and the effect of slime sheath which covers the entire slug, the boundary moves freely and the pressure p becomes zero on the boundary. Furthermore, the normal component of $\mathbf{J}_\alpha^\mathrm{rel}$ vanishes on the boundary, since cells do not leak out through the boundary.

3 Results

3.1 Stationary solution

First we will examine the cell-type distribution and overall shape of the slug at steady state. In a slug moving at a constant speed, cell mass at any position and the pacemaker should move at the same velocity, and the relative flux densities $\mathbf{J}_\alpha^\mathrm{rel}$ should vanish everywhere in the slug for all cell types. Under these conditions, we can obtain the stationary solution of the model.

We introduce a spherical polar coordinate system $\mathbf{r} = (r, \theta, \varphi)$, with its origin fixed at the position of the pacemaker, and assume that the slug moves at a constant velocity U in the direction that the polar angle θ is zero. Then the fraction of each cell type n_α at steady state satisfies the following equation:

$$a_\alpha D_\alpha \log n_\alpha + f_\alpha r + a_\alpha U r \cos\theta + \frac{p}{\rho} = c_\alpha, \tag{3}$$

where c_α is a constant determined by the total amount of type-α cells. Pressure $p(\mathbf{r})$ at position $\mathbf{r}$ is determined so that the relation $\sum_\alpha n_\alpha = 1$ holds (Appendix B).

Subtracting (3) for type-β cells from that for type-α cells, we have

$$\log \frac{{n_\alpha}^{a_\alpha D_\alpha}}{{n_\beta}^{a_\beta D_\beta}} + (f_\alpha - f_\beta) r + (a_\alpha - a_\beta) U r \cos\theta = c_\alpha - c_\beta, \tag{4}$$

which gives the relative abundance of cell type α and β at position $\mathbf{r}$. Equation (4) indicates that the quantities $H_\alpha(\theta) = f_\alpha + a_\alpha U \cos\theta$ for all cell types mainly determine the arrangement of cell types along the radial line at angle θ. A greater motive force favors the cells positioning closer to the pacemaker, whereas a large intrinsic resistance rate has the same effect as motive force for the cells positioned anterior to the pacemaker (i.e., $\cos\theta > 0$) and the opposite effect for the posterior cells ($\cos\theta < 0$). These effects are larger for the cells located on a radial line closer to the central axis, causing the spread of cells with large intrinsic resistance in the opposite direction to the slug migration.

If all the diffusion constants D_α are sufficiently small, different cell types will be segregated in the slug to form a clear sorting pattern. Then the boundary between the region of type-α cells and that of type-β cells can be defined as a surface on which $n_\alpha = n_\beta$ and $n_\alpha + n_\beta \simeq 1$, i.e., $n_\alpha = n_\beta \simeq 0.5$. Thus, the first term on the left-hand side of (4) becomes constant, and we have the following formula for the boundary shape:

$$r(\theta, \varphi) = \frac{C_{\alpha\beta}}{1 + \eta_{\alpha\beta} \cos\theta}, \tag{5}$$

where $\eta_{\alpha\beta} = (a_\alpha - a_\beta)U/(f_\alpha - f_\beta)$ and $C_{\alpha\beta}$ a constant. Equation (5) represents a surface of revolution obtained by rotating a conic section whose eccentricity is $\eta_{\alpha\beta}$ about the slug axis. The boundary is a spheroid if $|\eta_{\alpha\beta}| < 1$ or a paraboloid if $|\eta_{\alpha\beta}| = 1$ or a hyperboloid if $|\eta_{\alpha\beta}| > 1$. The pacemaker is positioned at a focus of the conic section. The shape of the entire slug can also be calculated from (3) in a similar way. Since $p = 0$ on the boundary, if the region of type-α cells is bordered by the outside of the slug, the boundary shape becomes the

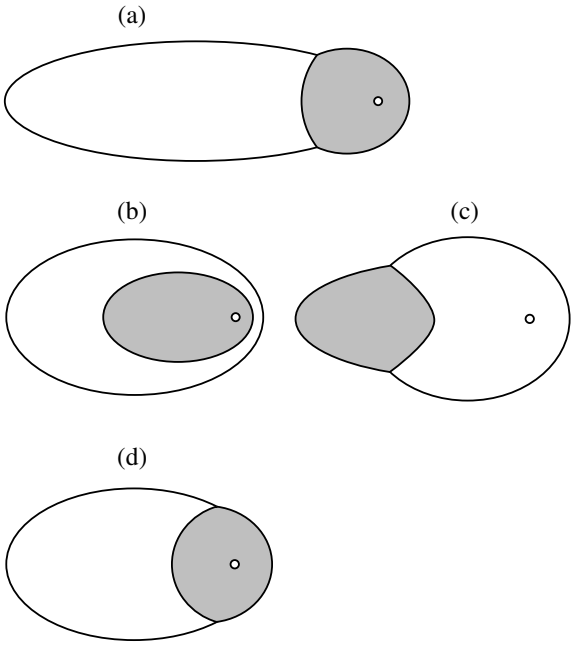

Fig. 1. Schematic diagram of the shapes of cell type regions and the entire slug consisting of two cell types. Longitudinal sections of axially symmetric slugs moving rightward are shown. Small white circle represents the position of the pacemaker. The slug volume is 1 and the ratio of type-A cells (grey) to type-B cells (white) is 1:4. Parameters are $f_{\mathrm{A}} = 2$, $f_{\mathrm{B}} = 1$, $a_{\mathrm{B}} = 1$ and (a) $a_{\mathrm{A}} = 1$, $U = 0.95$, (b) $a_{\mathrm{A}} = 2$, $U = 0.8$, (c) $a_{\mathrm{A}} = 3$, $U = 0.6$, (d) $a_{\mathrm{A}} = 1$, $U = 0.7$. Diffusion constants D_{A} and D_{B} are sufficiently small.

surface of revolution of a conic section whose eccentricity is $\eta_\alpha = a_\alpha U/f_\alpha$. In general, several cell types may face the boundary of the slug. Therefore, the boundary of the slug is formed by a combination of revolving conic sections.

To illustrate how the cell types divide the entire region of a slug in the stationary state, we consider an imaginary slug consisting of only two cell types, A and B. Figure 1 shows the boundary shapes at various sets of parameters. When type-A cells have greater motive force than type-B cells but the both have the same intrinsic resistance rate, type-A cells are positioned near the pacemaker and the slug shape becomes a combination of two intersecting spheroids. The boundary between the two cell types is a part of a sphere (Fig. 1a). This distribution pattern of cell types is the same as that considered in our previous study (Umeda and Inouye, 1999). When the resistance rate of type-A cells becomes greater than type-B cells, the boundary between the two cell types is elongated to become a spheroid. In the case of Fig. 1b, the region of type-A cells is completely surrounded by that of type-B cells. If the resistance rate of type-A cells becomes still larger, they will be displaced from the region around the pacemaker to the posterior region (Fig. 1c). In this case,

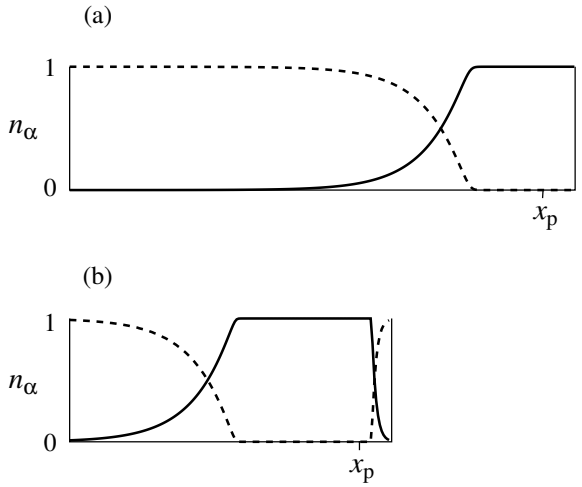

Fig. 2. Spatial distribution of cell types along the central axis of a slug. Fraction of type-A cells (solid line) and type-B cells (dashed line) are plotted against the distance from the bottom of the slug. x_p represents the position of the pacemaker. Parameters are (a) the same as Fig. 1a but $D_A = 0.2$, $D_B = 0.01$, (b) the same as Fig. 1b but $D_A = 0.02$, $D_B = 0.001$.

cell type boundary is not a spheroid but a hyperboloid.

In addition to the values of f and a, the boundary shape also depends on the velocity U. The slug shown in Fig. 1d has the same parameters as in Fig. 1a, but moves slower. These two figures indicate that as the slug velocity increases, the slug shape becomes more elongated and the position of the pacemaker is more distant from the middle of the slug. Conversely, as the pacemaker approaches the boundary of the slug, the slug moves faster. In our model, the relative position of the pacemaker, and consequently the velocity and the length of the slug at steady state, are determined by the initial distribution of cell types (see Section 3.3).

Next, we will examine the effects of the diffusion. The distributions of the two cell types along the axis of the same imaginary slugs shown in Fig. 1a and 1b, but now with diffusion ($D_A > D_B$) taken into consideration, were calculated from Eq. (4). As shown in Fig. 2, many type-A cells are distributed in the region where type-B cells are predominant (B-region), while the number of type-B cells present in the A-region is relatively small. This is because $a_A D_A > a_B D_B$. In general, cells that have larger value of $a_\alpha D_\alpha$ tend to disperse into the regions of other cells. The extent of cell dispersion is also affected by the slug movement. It can be seen in Fig. 2b that the cell type boundary positioned behind the pacemaker is more blurred than that before the pacemaker. This difference between the front and back side of the A-region in the degree of cell dispersion into the B-region becomes larger as the slug moves faster. These

facts can be understood because cells that have larger intrinsic resistance rate, namely type-A cells, tend to lag behind others.

3.2 Slug shape and cell positioning

Based on the above results, we consider the cell distribution patterns within real slugs. The slug of *D. discoideum* contains prespore cells and four types of prestalk cells (pstA, pstB, pstAB and pstO cells). PstA cells are normally distributed in the front of the prestalk region of a slug, and the rest of the prestalk region is mainly occupied by pstO cells. PstAB cells typically form a funnel-shaped cluster along the central axis near the tip of the slug. PstB cells and part of pstO cells are present in the prespore region, some forming loose clusters in the region in contact with the substratum as well as in the rearmost region (the latter being called rearguard cells) while others being scattered throughout the prespore region (called anterior-like cells) (Jermyn et al., 1996; Williams, 1997).

The shape of a 3-dimensional slug at steady state and the distribution of the prestalk cell subtypes and prespore cells within it can be calculated if the motive force, intrinsic resistance rate, diffusion coefficient, and relative abundance in the slug are given for each cell type. The motive force of prestalk cells and prespore cells can be estimated from the force measurement data of anterior and posterior fragments of migrating slugs and the spatial distribution of these cell types along the slugs (Inouye and Takeuchi, 1980). The intrinsic resistance rate of these cell types can be estimated by analysis of the quantitative data of slug migration (Inouye and Takeuchi, 1979). It has also been shown that the random component of cell movement is much larger in prestalk cells than in prespore cells (Kakutani and Takeuchi, 1986; Inagaki, 1992). Since the mechanical parameters of individual prestalk subtypes are not available, we performed numerical calculations using various combinations of plausible parameters to evaluate their effects on cell type distribution.

Figure 3 is an example of the shape and cell type distribution of a slug at steady state obtained with the set of parameters shown in Table 1. The overall shape of the slug as well as the distribution of prestalk subtypes and prespore cells are similar to those observed in real slugs. Particularly noteworthy are the shape of the pstAB domain leaving a trail, and the distribution of pstO cells, some of which form the coherent zone behind the pstA domain while the others are scattered in the prespore region. Furthermore, the variations of their spatial arrangement are very well reproduced in the model by modification of the parameters (not shown). These results support the hypothesis that the balance between the motive force and intrinsic resistance is central in determining the slug shape and cell positioning.

Table 1. Parameters used in the calculation of steady state distribution and in the simulation

cell type	f_α[1] [dyne]	a_α[2] [g/s]	$D_\alpha^{(3)}$ [μm^2/s]	fraction[4] [%]
pstAB	3.0×10^{-3}	22	1	3
pstA	2.6×10^{-3}	18	1	10
pstO	2.2×10^{-3}	18	3	14
pstB	0.5×10^{-3}	5	3	3
prespore	0.6×10^{-3}	6	0.1	70

1: the motive force of prestalk cells and prespore cells is estimated from the experimental data by Inouye and Takeuchi (1980) and the average volume per cell.
2: the intrinsic resistance rate of prestalk cells and prespore cells is obtained from the ratio between f and the velocity of a slug in which the resistance of slime sheath can be neglected (sufficiently large L in Eq. A of Inouye and Takeuchi (1979)).
3. D_α is neglected in the simulation (Fig. 4 and 5).
4: based on Hayashi and Takeuchi (1976); Sternfeld and David (1982); Gaskell et al. (1992) and author's unpublished data.

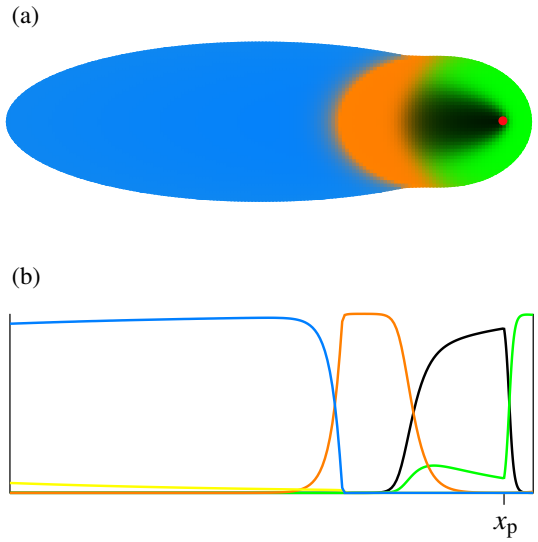

Fig. 3. Cell-type distribution in a model slug at stationary state. (a) longitudinal section, (b) fraction of cell types along the slug axis. Black: pstAB cells, green: pstA cells, orange: pstO cells, yellow: pstB cells, and blue: prespore cells. Red circle and x_p represent the position of the pacemaker. Slug velocity used for calculation is 0.95 [μm/s] and slug length 584 [μm]. Other parameters are shown in Table 1. Slug velocity is considerably larger than that of real slugs of the same length, because the effect of slime sheath is neglected in the calculation.

3.3 Simulation of slug formation

To obtain the exact changes in the cell distribution pattern and slug shape during slug development, the set of model equations (Eqs. (A.2) and (A.4)-(A.7) in Appendix A) must be solved for a given initial cell distribution. However, this is very difficult because the shape of the slug varies with time. Instead, we considered a group of cells and calculated the motion of these cells using Eq. (1) in the two-dimensional space. The continuous quantity ∇p in Eq. (1) was evaluated by using the MPS method (moving particle semi-implicit method), which was originally developed by Koshizuka and Oka (1996) to solve free boundary problems of incompressible fluid. Although the original calculation was based on the Navier-Stokes equations, the method can easily be applied to our problems (Appendix C).

Figure 4 shows an example of simulation, starting from a circular aggregate of 499 cells and a pacemaker positioned near the center of the aggregate. The aggregate comprises 5 cell types with the parameters shown in Table 1 except that diffusion is neglected. Starting from random distribution of all cell types, sorting of the majority of prestalk cells from prespore cells, shift of the prestalk region to one end of the aggregate, migration of the aggregate, and its elongation take place successively.

To see how cell sorting and morphogenetic movement progress, the velocity field of the aggregate was calculated by averaging the cell velocity over a small area at each point, and showed in Fig. 5 alongside snapshots of cell type distribution. Within 3 minutes, sorting between prestalk cells and prespore cells has been almost complete (Fig. 5a). In this stage the velocity $\mathbf{v}$ is almost zero everywhere in the aggregate. This indicates that the cell sorting occurs due to the relative flux density $\mathbf{J}_{\alpha}^{\mathrm{rel}}$. At 15 minutes, the pacemaker shifts from the center towards the right, and the entire cell mass begins to move in the same direction (Fig. 5b). The velocity $\mathbf{v}$ is greater in the central part of the cell mass, because cells in this region exerts greater motive force than the rest of cells. In other words, a convection flow arises within the cell mass due to the difference in motive force. This convection flow causes each cell type regions to move to their specific positions and the entire cell mass to change its shape. When the elongated shape of a slug is formed, the velocity of cell mass becomes almost constant everywhere (Fig. 5c), which was assumed in section 3.1 to obtain the stationary cell distribution and slug shape.

Several simulations starting with different configurations of cell positions gave similar results, although the slug lengths at steady state differed slightly. As stated previously, the slug velocity U at steady state, and consequently the final length of the slug, depend on the relative position of the pacemaker within the slug. Since the pacemaker moves as a result of the convection flow

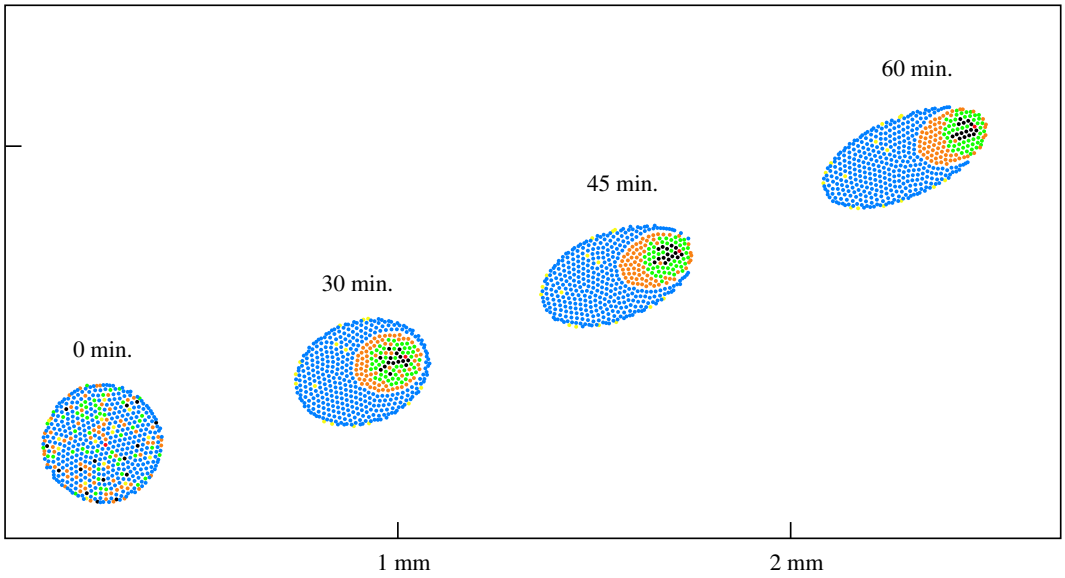

Fig. 4. An example of numerical calculation starting from a circular cell mass. Black: pstAB cells, green: pstA cells, orange: pstO cells, yellow: pstB cells, blue: prespore cells, and red: the pacemaker. Parameters f_α and a_α for each cell type are shown in Table 1. Other parameters are $dt = 0.5$ [s], $r_e = 0.04$ [mm], $n^0 = 20$, $\beta = 0.97$.

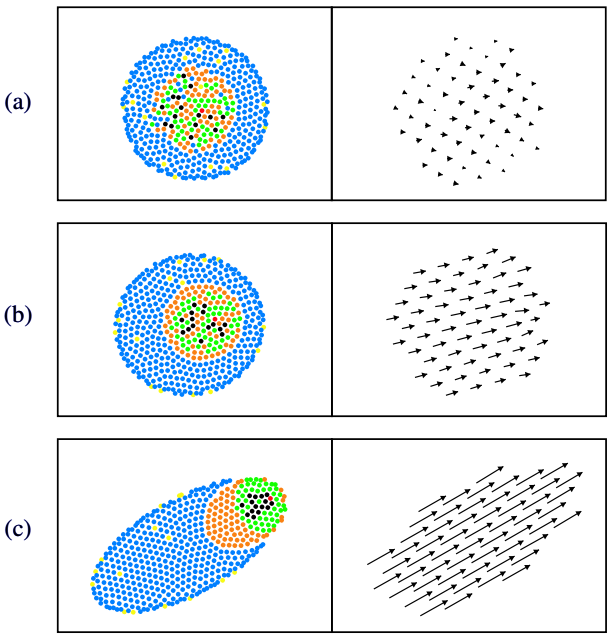

Fig. 5. Cell type distribution and the velocity of cell mass at the indicated times are shown. (a) 3 [min], (b) 15 [min], (c) 120 [min].

of aggregate and the velocity of cell mass is determined by the distribution of cell types, the final position of the pacemaker generally depends on the initial cell distribution. However, when a simulation is started from a circular aggregate with the pacemaker at its center, and with randomly distributed cell types, the final shape of slugs was almost identical. Since the pacemaker is normally positioned at the center of cell mass after cell aggregation, initial conditions will make little difference in slug shape.

4 Discussion

In the present study, formation of the elongated shape of *Dictyostelium* slugs and cell positioning within them were investigated using a simple mathematical model based on the balance of mechanical forces. Examination of stationary solutions of the model indicated that not only the 3-dimensional prestalk-prespore distribution but the distributions of the prestalk sub-populations can also be accounted for by the differences in mechanical properties of cells between different cell types. Computer simulations of the process of slug formation in 2-dimensional space reproduced many of the basic features of slug morphogenesis, i.e., cell sorting, translocation of the pacemaker and the prestalk region, elongation of the slug, and its steady migration. The cell-type distributions within the slugs were very similar to the one at steady state obtained analytically using the same set of parameters.

The idea that cell motility differences between cell types may account for their positions within the slug (Bonner, 1952) has been tested by various types of mathematical models and shown to be a plausible mechanism for the formation of the prestalk-prespore pattern (Dormann et al., 1998; Vasiev and Weijer, 1999; Umeda and Inouye, 1999; Pálsson and Othmer, 2000). In these studies, however, only the difference in chemotactic force is taken into consideration as a possible cause of cell motility difference, and no distinction is made between prestalk subtypes. In the present study, the prestalk subtypes have been incorporated in the model, and the difference in the intrinsic resistance rate between cell types was taken into consideration. Mathematical analysis indicated that the motive force and the intrinsic resistance rate have different effects on the positioning of cell types. While the effects of the motive force on the cell-type distribution depend solely on the distance from the pacemaker, the effects of the intrinsic resistance rate relate to the magnitude and the direction of the slug velocity. For instance, in an elongated slug migrating at a large velocity, a cell type with large motive force and large intrinsic resistance rate would accumulate around the pacemaker, due to the large value of f, but at the same time tend to show a distribution pattern with a trailing tail along the axis of the slug, due to the large a and U. Such a distribution pattern is typically observed with pstAB cells in real slugs.

We also examined the effect of the diffusion of cells, and obtained results which may explain the scattered cell distribution especially seen in anterior-like cells. The diffusion term of the model was derived from random force, which may include the disturbance of motive force as well as external noise. Within real slugs, the presence of the random components of the motive force would give rise to temporal fluctuations of cell speeds. Such fluctuations have been observed in real migrating slugs (Kakutani and Takeuchi, 1986). Quantitative measurements of the changes in cell positions in migrating slugs indicate that prestalk cells show much larger velocity fluctuations, and therefore much larger diffusion constant, than prespore cells (Inagaki, 1992). This may explain why some prestalk cells (mostly pstO cells because they share a border with the prespore region) are distributed deep in the prespore region whereas prespore cells hardly ever invade the prestalk region. As shown in Figure 2, the extent of cell dispersion is also affected by the intrinsic resistance rate and the slug movement. Besides the larger diffusion constant, larger intrinsic resistance of prestalk cells than prespore cells will enhance the dispersion of prestalk cells. In the case of pstAB cells, their tendency to lag behind along the slug axis due to the large intrinsic resistance rate would be enhanced as the slug moves faster.

In addition to these effects of the random components of the motive force, heterogeneity in f and a within each cell type may contribute to the scattered distribution of anterior-like cells. Within the region posterior to the pacemaker, the cell type distribution near the central axis is determined by the values of $H_\alpha(\pi) = f_\alpha - a_\alpha U$. Therefore, pstAB cells and pstO cells that have $H(\pi)$ values almost equivalent to the mean $H(\pi)$ of prespore cells will be scattered in the prespore region. On the other hand, some of the pstAB cells lag behind during migration and eventually lost from the slug (Sternfeld, 1992). This phenomenon may be interpreted as a result of the decreasing $H(\pi)$ value due either to a decrease in f or to an increase in a. Furthermore, the entire process of stalk formation can be seen as a sequential motility loss of prestalk cells under strict control, because the loss of motility can be formulated as a decline in the motive force and/or increase in the intrinsic resistance rate (see Fig. 1c).

As to the pattern formation in *Dictyostelium*, differential cell adhesion has also been considered as a possible mechanism of cell sorting. Although cell adhesion alone would not account for the morphogenetic movement of slugs, some simulation studies have shown that cooperation of differential adhesion and chemotaxis is capable of reproducing the slug formation and migration (Yi Jiang et al., 1998; Marée et al., 1999; Pálsson and Othmer, 2000). Our model implicitly incorporates cell adhesion, because the cell density is assumed to be constant and the motive force generated by cells to be transmitted to the substratum via cell-cell contact (Umeda and Inouye, 1999). However, possible differences in adhesiveness between cell types are ignored in the model. The

fact that the model reproduced many of the basic features of slug morphogenesis suggests that differential adhesion is not an essential component as far as major aspects of morphogenesis and patterning in *Dictyostelium* are concerned. Viscous drag force between cells, which has been assumed in some mechanical models (Odell and Bonner, 1986; Pálsson and Othmer, 2000), is also not considered in the model. The lateral cell cortices of apposing cells adhere to each other and there is no slip between the cortices while the main body of the cells moves (Umeda and Inouye, 1999).

One advantage of the present model is its simplicity. The model has a stationary solution calculated from Eq. (3), which enabled us to analyze how each parameter of the model determine the cell positioning without the help of simulation studies. On the other hand, some of the important factors that relate to the microscopic cell motion may be ignored in the model formulation. We regarded the pacemaker as a point moving with the average speed of the surrounding cells and assumed that chemotactic signals propagate instantly and uniformly from this point. However, the signals are mediated by excitable cells and their speed may vary with cell types or the environmental condition of cells. The position of the pacemaker can shift due to the random force of the surrounding cells. These factors may affect the movement of individual cells and would change the distribution pattern of cell types in consequence, as have been demonstrated by some individual-based models (Marée et al., 1999; Pálsson and Othmer, 2000; Marée and Hogeweg, 2001). Contact following is another important factor that affects cell movement, such as causing rotational motion of cells in slugs (Umeda and Inouye, 2002). Incorporation of these effects into the model may produce more realistic behavior of mounds and slugs.

A test of the proposed model would be to determine the motive force and intrinsic resistance rate of each cell type by measuring changes in the velocity of isolated cells under controlled external force. A motility assay of isolated *Dictyostelium* cells under external force has been reported (Laevsky and Knecht, 2001). Considering the possible effects of isolation on cell motility, however, it is also important to estimate the mechanical properties of cells in tissues. This may be achieved by carefully observing the distribution of cell types within slugs migrating under various magnitudes of external force. Hydrostatic pressure (Inouye and Takeuchi, 1980) and centrifugal force (Inouye, 1984) have been successfully used for application of external force on migrating slugs. Our model predicts that the cells located posterior to the pacemaker of an elongated slug will be arranged in order of $f_\alpha - a_\alpha U$ along its axis. Therefore, a change in U will have different effects on the distribution of cell types that have different a_α. The model further predicts that the distribution of cell types along a line perpendicular to the slug axis depends solely on f_α irrespective of the slug speed. On the other hand, the diffusion coefficient of cells would be determined by quantitative measurements of position changes of individ-

ual cells within migrating slugs. We are planning experiments to determine these variables and examine how they are related to the cell-type positioning in *Dictyostelium*.

Acknowledgements

This research was supported in part by Grant-in-Aid for Scientific Research (c)-11837011 from Japan Society for the Promotion of Science to T.U.

Appendix A: Model formulation

In this appendix, we describe the mathematical formulation of the model. We consider a slug consisting of several cell types. A type-α cell in the slug moves with the velocity $\mathbf{V}_\alpha$ which is determined by Eq. (1). Since both oriented movement and the diffusion of cells contribute to the flow of cells, the flux density of type-α cells may be written as

$$\mathbf{J}_\alpha = \rho n_\alpha \langle \mathbf{V}_\alpha \rangle - \rho \sum_\beta D_{\alpha\beta} \nabla n_\beta, \tag{A.1}$$

where the angle brackets denote the average value. Diffusion coefficients $D_{\alpha\beta}$ in general depend on the fractions of all cell types. For simplicity, we hereafter neglect $D_{\alpha\beta}$ for $\beta \neq \alpha$ and assume that $D_\alpha = D_{\alpha\alpha}$ is constant. Then substituting (1) into (A.1) gives

$$\mathbf{J}_\alpha = \frac{\rho f_\alpha n_\alpha}{a_\alpha} \frac{\mathbf{x}_\mathrm{p} - \mathbf{x}}{|\mathbf{x}_\mathrm{p} - \mathbf{x}|} - \frac{n_\alpha}{a_\alpha} \nabla p - \rho D_\alpha \nabla n_\alpha, \tag{A.2}$$

and the changes in the fraction of cell type are governed by

$$\rho \frac{\partial n_\alpha}{\partial t} = -\nabla \cdot \mathbf{J}_\alpha. \tag{A.3}$$

We define the velocity of the cell mass at position $\mathbf{x}$ at time t as

$$\mathbf{v}(\mathbf{x}, t) = \frac{1}{\rho} \sum_\alpha \mathbf{J}_\alpha. \tag{A.4}$$

Then summing up (A.3) and using $\sum_\alpha n_\alpha = 1$ give

$$\nabla \cdot \mathbf{v} = 0. \tag{A.5}$$

If we use the relative flux density $\mathbf{J}_\alpha^{\mathrm{rel}} = \mathbf{J}_\alpha - \rho n_\alpha \mathbf{v}$, (A.3) can be rewritten as

$$\rho \left[\frac{\partial n_\alpha}{\partial t} + \mathbf{v} \cdot \nabla n_\alpha \right] = -\nabla \cdot \mathbf{J}_\alpha^{\mathrm{rel}}. \tag{A.6}$$

Equations (A.4) and (A.5) determine the velocity and the pressure distribution in the slug, and (A.6) governs the changes in the fraction of cell types.

On the boundary of the slug, the normal component of $\mathbf{J}_\alpha^{\mathrm{rel}}$ vanishes. Furthermore if we neglect the force from the substratum and the effect of the slime sheath, the boundary moves freely and the pressure p becomes zero on the boundary.

Finally, the position of the pacemaker is determined by

$$\frac{d\mathbf{x}_{\mathrm{p}}}{dt} = \mathbf{v}(\mathbf{x}_{\mathrm{p}}, t), \tag{A.7}$$

since the pacemaker moves with the surrounding cells.

Appendix B: Stationary solution

The stationary solution of the model can be obtained if we assume that cell mass at any position of a slug moves with the same constant velocity.

Let $\mathbf{U}$ be a constant vector and $\mathbf{r} = \mathbf{x} - \mathbf{x}_{\mathrm{p}}$. Then $\mathbf{r}/r = \nabla r$ and $\mathbf{U} = \nabla(\mathbf{U} \cdot \mathbf{r}) = \nabla(Ur\cos\theta)$, where $r = |\mathbf{r}|$, $U = |\mathbf{U}|$, and θ the angle between $\mathbf{U}$ and $\mathbf{r}$. Thus, if the cell mass moves with $\mathbf{U}$, the relative flux density $\mathbf{J}_\alpha^{\mathrm{rel}} = \mathbf{J}_\alpha - \rho n_\alpha \mathbf{U}$ becomes

$$\mathbf{J}_\alpha^{\mathrm{rel}} = -\frac{\rho n_\alpha}{a_\alpha} \nabla \left[a_\alpha D_\alpha \log n_\alpha + f_\alpha r + a_\alpha U r \cos\theta + \frac{p}{\rho} \right]. \tag{B.1}$$

Since $\mathbf{J}_\alpha^{\mathrm{rel}}$ vanishes everywhere in the slug at steady state, (B.1) leads to

$$a_\alpha D_\alpha \log n_\alpha + f_\alpha r + a_\alpha U r \cos\theta + \frac{p}{\rho} = c_\alpha, \tag{B.2}$$

where c_α is a constant determined by the total amount of type-α cells.

Solving (B.2) for n_α and substituting it into $\sum_\alpha n_\alpha = 1$,

$$\sum_\alpha \exp\left[\frac{c_\alpha - f_\alpha r - a_\alpha U r\cos\theta - p/\rho}{a_\alpha D_\alpha}\right] = 1, \tag{B.3}$$

from which pressure distribution $p(\mathbf{r})$ can be obtained. Then Eq. (B.2) gives $n_\alpha(\mathbf{r})$ for each cell type. The slug occupies the domain that satisfies $p(\mathbf{r}) \geq 0$.

A Appendix C: Numerical method

The numerical simulation is performed by calculating the motion of individual cells. Neglecting the random forces, Eq. (1) means that the movement of the ith cell is governed by the following equation:

$$\frac{d\mathbf{x}_i}{dt} = \frac{f_i}{a_i}\frac{\mathbf{x}_\mathrm{p} - \mathbf{x}_i}{|\mathbf{x}_\mathrm{p} - \mathbf{x}_i|} - \frac{1}{\rho a_i}\nabla p. \tag{C.1}$$

To evaluate the continuous quantities such as pressure gradient, we introduce a kernel function

$$w(r) = \begin{cases} r_e/r - 1 & (0 < r < r_e) \\ 0 & (r_e \leq r) \end{cases}, \tag{C.2}$$

where r_e is the range of cell interaction. Then, cell density at the position $\mathbf{x}_i$ of cell i may be proportional to

$$\langle n\rangle_i = \sum_{j\neq i} w(|\mathbf{x}_j - \mathbf{x}_i|). \tag{C.3}$$

Incompressibility of cell mass requires that $\langle n\rangle_i$ for all cells in the slug should have a constant value n^0. If cell i possesses the value of pressure p_i, the gradient and Laplacian of p at cell i, respectively, are approximated by

$$\langle \nabla p\rangle_i = \frac{d}{n^0}\sum_{j\neq i}\left[\frac{p_j - p_i'}{|\mathbf{x}_j - \mathbf{x}_i|^2}(\mathbf{x}_j - \mathbf{x}_i)w(|\mathbf{x}_j - \mathbf{x}_i|)\right] \tag{C.4}$$

and

$$\langle \nabla^2 p\rangle_i = \frac{2d}{n^0\lambda}\sum_{j\neq i}(p_j - p_i)w(|\mathbf{x}_j - \mathbf{x}_i|), \tag{C.5}$$

where d is the number of space dimension and $\lambda = \int w(r)r^2 dv \,/ \int w(r)dv$. In (C.4), $p'_i = \min(p_j)$ for j satisfying $w(|\mathbf{x}_j - \mathbf{x}_i|) \neq 0$ is used instead of p_i, in order to stabilize the calculation (Koshizuka and Oka, 1996).

Equations (C.1) are solved as follows. First, positions of cells are updated according to

$$\mathbf{x}'_i = \mathbf{x}_i + \frac{\Delta t f_i}{a_i} \frac{\mathbf{x}_\mathrm{p} - \mathbf{x}_i}{|\mathbf{x}_\mathrm{p} - \mathbf{x}_i|}. \tag{C.6}$$

Then, (C.3) is calculated for all cells including the pacemaker. In this stage, $\langle n \rangle_i$ is not equal to n^0. Continuation equation $\partial n/\partial t = 0$ requires the following Poisson equation of pressure:

$$\langle \nabla^2 p \rangle_i = -\frac{\rho}{\Delta t \langle 1/a \rangle} \frac{\langle n \rangle_i - n^0}{n^0}, \tag{C.7}$$

where $\langle 1/a \rangle$ is the weighted average of $1/a_i$. A cell satisfying $\langle n \rangle_i < \beta n^0$ is regarded as a cell on the slug boundary, where β is a parameter below 1.0. Pressure zero is given to such cells, and the values of pressure for the rest of the cells and the pacemaker are calculated using the Poisson equation (C.7) and (C.5). Cell positions are then modified according to

$$\mathbf{x}''_i = \mathbf{x}'_i - \Delta t \frac{\langle \nabla p \rangle_i}{a_i \rho}. \tag{C.8}$$

Finally, the position of the pacemaker is updated by

$$\mathbf{x}'_\mathrm{p} = \mathbf{x}_\mathrm{p} + \frac{\sum_j (\mathbf{x}''_j - \mathbf{x}_j) w(|\mathbf{x}_j - \mathbf{x}_\mathrm{p}|)}{\sum_j w(|\mathbf{x}_j - \mathbf{x}_\mathrm{p}|)}. \tag{C.9}$$

References

Araki, T., Abe, T., Williams, J. G., Maeda, Y., 1997. Symmetry breaking in *Dictyostelium* morphogenesis: evidence that a combination of cell cycle stage and positional information dictates cell fate. Dev. Biol. 192, 645-648.

Bonner, J. T., 1952. The pattern of differentiation in amoeboid slime molds. Am. Naturalist 86, 79-89.

Bonner, J. T., 1994. The migration stage of *Dictyostelium*: behavior without muscles or nerves. (minireview). FEMS Microbiol. Lett. 120, 1-8.

Dormann, D., Vasiev, B., Weijer, C. J., 1998. Propagating waves control *Dictyostelium discoideum* morphogenesis. Biophys. Chem. 72, 21-35.

Dormann, D., Vasiev, B., Weijer, C. J., 2000. The control of chemotactic cell movement during *Dictyostelium* morphogenesis. Phil. Trans. R. Soc. Lond. B 355, 983-991.

Early, A., Abe, T., Williams, J. G., 1995. Evidence for positional differentiation of prestalk cells and for a morphogenetic gradient in *Dictyostelium*. Cell 83, 91-99.

Feit, I. N., Bonner, J. T., Suthers, H. B., 1990. Regulation of the anterior-like cell state by ammonia in *Dictyostelium discoideum*. Dev. Genet. 11, 442-446.

Gaskell, M. J., Jermyn, K. A., Watts, D. J., Treffry, T., Williams, J. G., 1992. Immunolocalization and separation of multiple prestalk cell types in *Dictyostelium*. Differentiation 51, 171-176.

Hayashi, M., Takeuchi, I., 1976. Quantitative analysis on cell differentiation during morphogenesis of the cellular slime mold *Dictyostelium discoideum*. Dev. Biol. 50, 302-309.

Inagaki, Y., 1992. Analysis of cell movement in migrating slugs of *Dictyostelium discoideum*. (in Japanese). Master's Thesis, Kyoto University.

Inouye, K., 1984. Measurement of the motive force of the migrating slug of *Dictyostelium discoideum* by a centrifuge method. Protoplasma 121, 171-177.

Inouye, K., Takeuchi, I., 1979. Analytical studies on migrating movement of the pseudoplasmodium of *Dictyostelium discoideum*. Protoplasma 99, 289-304.

Inouye, K., Takeuchi, I., 1980. Motive force of the migrating pseudoplasmodium of the cellular slime mould *Dictyostelium discoideum*, J. Cell. Sci. 41, 53-64 .

Jermyn, K., Traynor, D., Williams, J., 1996. The initiation of basal disc formation in *Dictyostelium discoideum* is an early event in culmination. Development 122, 753-760.

Kakutani, T., Takeuchi, I., 1986. Characterization of anterior-like cells in *Dictyostelium* as analyzed by their movement. Dev. Biol. 115, 439-445.

Koshizuka, S., Oka, Y., 1996. Moving-particle semi-implicit method for fragmentation of incompressible fluid. Nucl. Sci. Eng. 123, 421-434.

Laevsky, G., Knecht, D. A., 2001. Under-agarose folate chemotaxis of *Dictyostelium discoideum* amoebae in permissive and mechanically inhibited

conditions. BioTechniques 31, 1140–1149.

Marée, A. F. M., Panfilov, A. V., Hogeweg, P., 1999. Migration and thermotaxis of *Dictyostelium discoideum* slugs, a model study. J. Theor. Biol. 199, 297-309.

Marée, A. F. M., Hogeweg, P., 2001. How amoeboids self-organize into a fruiting body: Multicellular coordination in *Dictyostelium discoideum*. Proc. Natl. Acad. Sci. USA 98, 3879-3883.

Odell, G. M., Bonner, J. T., 1986. How the *Dictyostelium discoideum* grex crawls. Phil. Trans. R. Soc. 312, 487-525.

Pálsson, E., Othmer, H. G., 2000. A model for individual and collective cell movement in *Dictyostelium discoideum*. Proc. Natl. Acad. Sci. USA 97, 10448-10453.

Sternfeld, J., David, C. N., 1982. Fate and regulation of anterior-like cells in *Dictyostelium* slugs. Dev. Biol. 93, 111-118.

Sternfeld, J., 1992. A study of pstB cells during *Dictyostelium* migration and culmination reveals a unidirectional cell type conversion process. Roux's Arch. Dev. Biol. 201, 354-363.

Tasaka, M., Takeuchi, I., 1981. Role of cell sorting in pattern formation in *Dictyostelium discoideum*. Differentiation18,191-196.

Umeda, T., 1989. A mathematical model for cell sorting, migration and shape in the slug stage of *Dictyostelium discoideum*. Bull. Math. Biol. 51, 485-500.

Umeda, T., Inouye, K., 1999. Theoretical model for morphogenesis and cell sorting in *Dictyostelium discoideum*. Physica D 126, 189-200.

Umeda, T., Inouye, K., 2002. Possible role of contact following in the generation of coherent motion of *Dictyostelium* cells. J. Theor. Biol. 219, 301-308., doi:10.1006/yjtbi.3124.

Vasiev, B., Weijer, C. J., 1999. Modeling chemotactic cell sorting during *Dictyostelium discoideum* mound formation. Biophys. J. 76, 595-605.

Williams, J. G., 1997. Prestalk and stalk cell heterogeneity in *Dictyostelium*, in Maeda, Y., Inouye, K., Takeuchi, I. (Eds.), *Dictyostelium* - A model system for cell and developmental biology, Universal Academy Press, Tokyo, Japan, pp. 293-304.

Williams, J. G., Duffy, K. T., Lane, D. P., McRobbie, S. J., Harwood, A. J., Traynor, D., Kay, R. R., Jermyn, K. A., 1989. Origins of the prestalk-prespore pattern in *Dictyostelium* development. Cell 59, 1157-1163.

Yi Jiang, Levine, H., Glazier, J., 1998. Possible cooperation of differential adhesion and chemotaxis in mound formation of *Dictyostelium*. Biophys. J. 75, 2615-2625.